Title

The Importance of the Lithium Ion Transference Number in Lithium/Polymer Cells

Authors

Doyle, M
Fuller, T F
Newman, J

Publication Date

1993-07-01

LBL34378
UC-331
Preprint

Lawrence Berkeley Laboratory
UNIVERSITY OF CALIFORNIA

Materials Sciences Division

Submitted to Electrochimica Acta

The Importance of the Lithium Ion Transference Number in Lithium/Polymer Cells

M. Doyle, T. F. Fuller and J. Newman

July 1993

Prepared for the U.S. Department of Energy under Contract Number DE-AC03-76SF00098

DISCLAIMER

LBL-34378
UC-331

The Importance of the Lithium Ion Transference Number in Lithium/Polymer Cells

Marc Doyle, Thomas F. Fuller, and John Newman

Department of Chemical Engineering
University of California

and

Materials Sciences Division
Lawrence Berkeley Laboratory
University of California
Berkeley, California 94720

July 1993

This work was supported in part by the Assistant Secretary for Conservation and Renewable Energy, Office of Transportation Technologies, Electric and Hybrid Propulsion Division of the U. S. Department of Energy under Contract No. DE-AC03-76SF00098.

The Importance of the Lithium Ion Transference Number in Lithium/Polymer Cells

Marc Doyle, Thomas F. Fuller, and John Newman

Department of Chemical Engineering
University of California
and
Materials Sciences Division
Lawrence Berkeley Laboratory
Berkeley, California 94720

Abstract

Simulation results are presented for a lithium negative electrode, solid polymer separator, manganese dioxide composite positive electrode cell. In particular, we assess the effect of conductivity and transference number on cell performance, establishing criteria for situations when a tradeoff between these two properties is expected. We show that polymer-electrolyte systems with a unity transference number have greatly improved performance over systems with t_+^0=0.2, even when the conductivity is decreased by an order of magnitude. The improvements are primarily at higher rates of discharge, where the latter cell would be depleted of electrolyte due to large concentration gradients that develop. Cells with a unity transference number have larger energy densities and can attain higher peak-power densities.

Key words: lithium, polymer electrolyte, transference number, modeling, battery

Introduction

Solid polymer electrolytes are being contemplated for use in rechargeable lithium batteries, where the advantages of an all-solid-state system have been demonstrated.[1] A lot of attention has been given to the consequences of a nonunity transference number of the lithium ion in lithium salt/polymer solutions. Most attempts to measure the transference number in lithium salt/polymer systems have led to considerable variation in their results. However, it is generally accepted that the transference number of the lithium ion is less than 0.5.[2,3] It has been recognized that such a value does not preclude the development of a successful lithium battery. Nevertheless, there is still much concern about the detrimental effect of large concentration gradients that necessarily develop during operation of the cell. Other than an increase in concentration polarization, there are also depletion of the electrolyte in the back of the porous electrodes and solubility limitations to be considered.

One strategy to increase the lithium ion transference number is to graft the anion onto the backbone of the polymer chain.[4-8] This leads to a unity transference number for the lithium ion as the mobility of the anion is zero. A related method is the use of very large, and hence relatively immobile, anions.[9] Unfortunately, immobilizing the anion typically results in large decreases in the ionic conductivity of the lithium salt/polymer solution. This decrease in conductivity is attributed to the role that anion motion plays in the conduction mechanism in these polymers. For example, in lithium salt/polyethylene oxide (PEO) solutions, it is suggested that a coordinated anion motion is required

to allow the lithium ion to "hop" along ether oxygen sites.[10] When the anion is covalently bound to the polymer chain, the decrease in conductivity has been significantly larger than expected from dilute solution theory. The conductivity of a dilute binary salt solution,

$$\kappa = \frac{F^2 c}{RT}\left(z_+^2 D_+ + z_-^2 D_-\right) , \tag{1}$$

would predict an 80% decrease in conductivity for a system initially having t_+=0.2.[11]

It is useful to take a moment to define clearly the transference number used in this work. Because of the failure of dilute solution theory for lithium salt/polymer electrolyte solutions, we will use the more rigorous concentrated solution theory. Under concentrated solution theory, transport processes are described by $n(n-1)/2$ pairwise interaction parameters D_{ij}, where n is the number of independent species. These parameters can be related to measureable transport properties.[11] For a binary salt in a polymer solvent, the transference number is related to the D_{ij} through the expression

$$t_+^0 = 1 - t_-^0 = \frac{z_+ D_{0+}}{z_+ D_{0+} - z_- D_{0-}} , \tag{2}$$

Here the transference number is defined with respect to the solvent species, thus the superscript 0. The transference number is exactly zero for neutral species, in contrast to the transport number, t_j^i/z_j, which may be nonzero, as has been demonstrated.[11] It is possible with this approach for t_+^0 to be less than zero, which has been demonstrated to result from a selection of species for the macroscopic model not

reflecting the actual species existing in solution at a given concentration.[12] The consequences of a transference number of less than zero will be discussed hereinafter.

We have developed a model to simulate the behavior of the lithium/polymer/insertion cell.[13] The model uses concentrated solution theory with variable transport properties to describe the lithium salt/polymer solution. A summary of the model equations is given in appendix A. Using this model, we can simulate the effect of a unity transference number on the performance of the system. This should allow us to develop criteria to assess the tradeoff between ohmic drop and concentration overpotential that results from the unity transference number. In addition, for a particular system we can determine the minimum value of the conductivity that still leads to an improvement in the performance of the system. This work should be helpful to researchers attempting to develop improved polymer solvents for lithium batteries.

Results and Discussion

We modeled a cell consisting of a solid lithium negative electrode, a lithium salt in a polymer solvent, and a manganese dioxide positive electrode (figure 1). The positive electrode is a porous composite electrode consisting of active manganese dioxide particles, inert conducting material such as carbon black, and the solution phase, each of known volume fraction. The electronic conductivity of the positive electrode is assumed to be large (100 S/m), so that ohmic drop in the electrode is not important. In addition, a large kinetic rate constant is assumed for the insertion process, corresponding to $i_{o,2}$=156 A/m^2 at

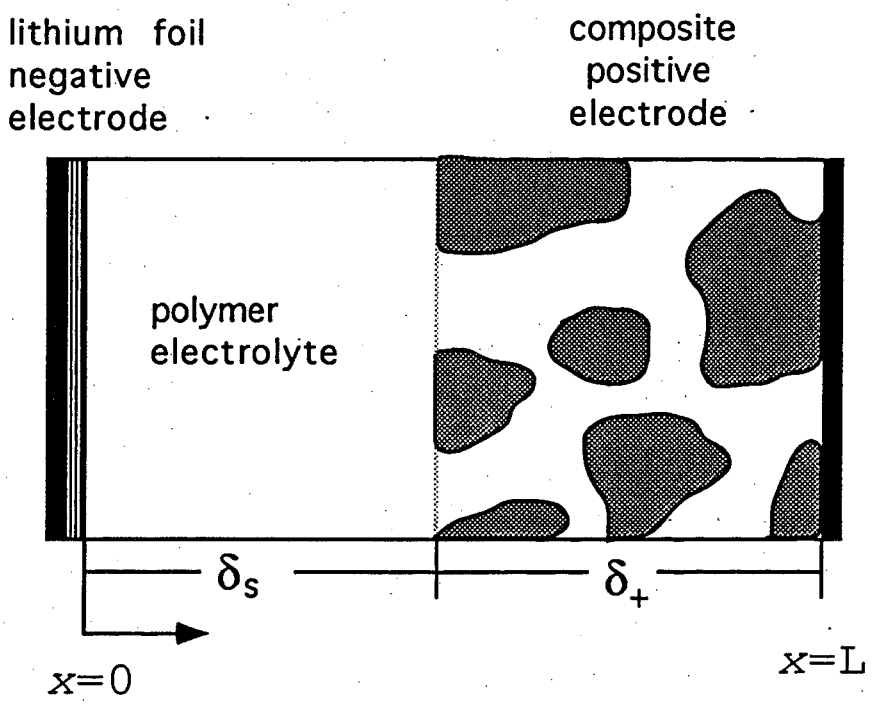

Figure 1. Lithium/polymer cell sandwich, consisting of lithium-foil negative electrode, solid-polymer electrolyte, and composite manganese dioxide positive electrode.

the initial conditions.

Table 1.

Parameters used in the simulation

System specific			Adjustable	
parameter	value	Ref.	parameter	value
D_s	1.0×10^{-13} m^2/s	14	T	100°C
σ	100 S/m	-	δ_s	50 μm
$i_{o,1}$	12.6 A/m^2	15,*	δ_+	100 μm
α_a,α_c	0.5	‡	R_s	1.0 μm
ν_+,ν_-	1	-	c^o	1000 mol/m^3
c_t	23,720 mol/m^3	-	ϵ	0.3
n	1	-	ϵ_f	0.151
ρ_s	4100 kg/m^3	-	-	-

The simulations to follow will be separated into two sections: the first are simulation results for a common system with transport properties taken from the literature. The electrolyte is $LiCF_3SO_3$ (lithium triflate) in polyethylene oxide (PEO), due to the relative abundance of data on this system. This first simulation will be the only system with a nonunity transference number and will represent a base case for comparison with later simulations. The second set of simulations is for the same system, but with a transference number of unity and the conductivity varied over a specified range. For simulations in which t_+^0=1.0, no concentration gradients exist in the solution phase, and variable

‡ Data are not available for these parameters.

* Value given is at initial conditions.

transport properties are not necessary.

Additional parameters used in this model are listed in table 1. Manganese dioxide has been demonstrated to insert lithium over a wide range of compositions, corresponding to $0.2<y<2.0$ in $Li_yMn_2O_4$. However, in this simulation we use only the upper plateau, giving a range of $0.2<y<1.0$. Therefore, the maximum concentration in the positive electrode is estimated from the density of the material at composition $LiMn_2O_4$.

Figure 2 gives the cell potential with respect to a lithium reference electrode at various discharge rates. The dashed line is the open-circuit potential (see appendix B). Transport properties for this salt/solvent system are also given in appendix B. Relevant to the present work, the transference number in this system is about 0.19 at the initial concentration. At higher rates of discharge, large concentration gradients are established in the cell, depleting the electrolyte in the back of the composite cathode for $I>2$ A/m^2. Once the concentration is driven to zero in the electrode, the active material in regions further to the back can no longer be utilized. This is the reason that discharge curves at $I=5$ and 10 A/m^2 drop off at less than 100% utilization of active material.

The depletion of the electrolyte can be seen clearly in figure 3, which gives concentration profiles in the solution phase at several times during a discharge at $I=5$ A/m^2. A large concentration gradient quickly develops in the positive electrode, and very little material is able to diffuse into the back of the electrode. Thus, once the material initially in the back has been inserted, the concentration is driven to

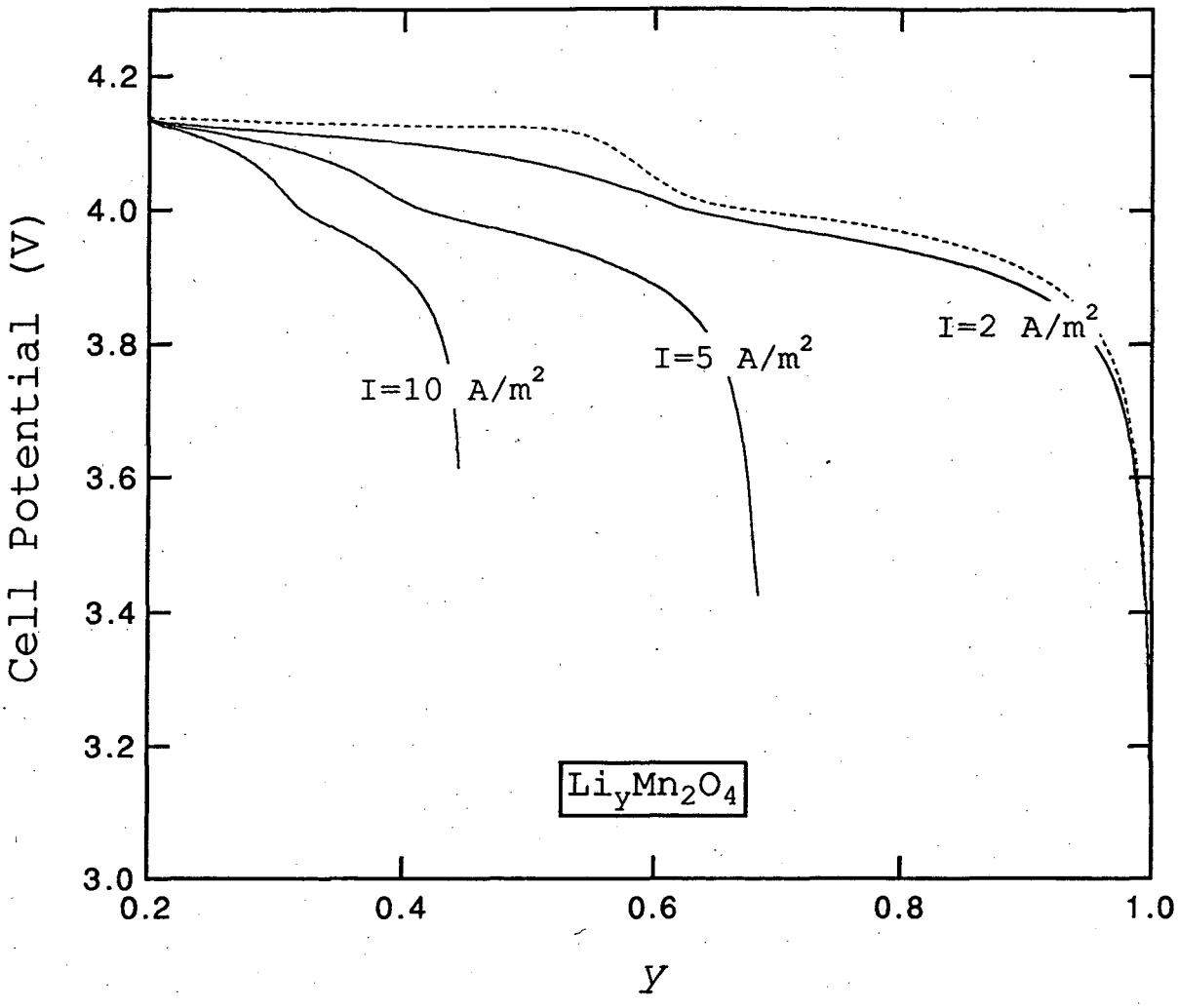

Figure 2. Cell potential *versus* state of charge for the lithium/manganese dioxide system at various discharge rates. The dashed line is the open-circuit potential of the cell. Other parameters used in the simulations are given in table 1.

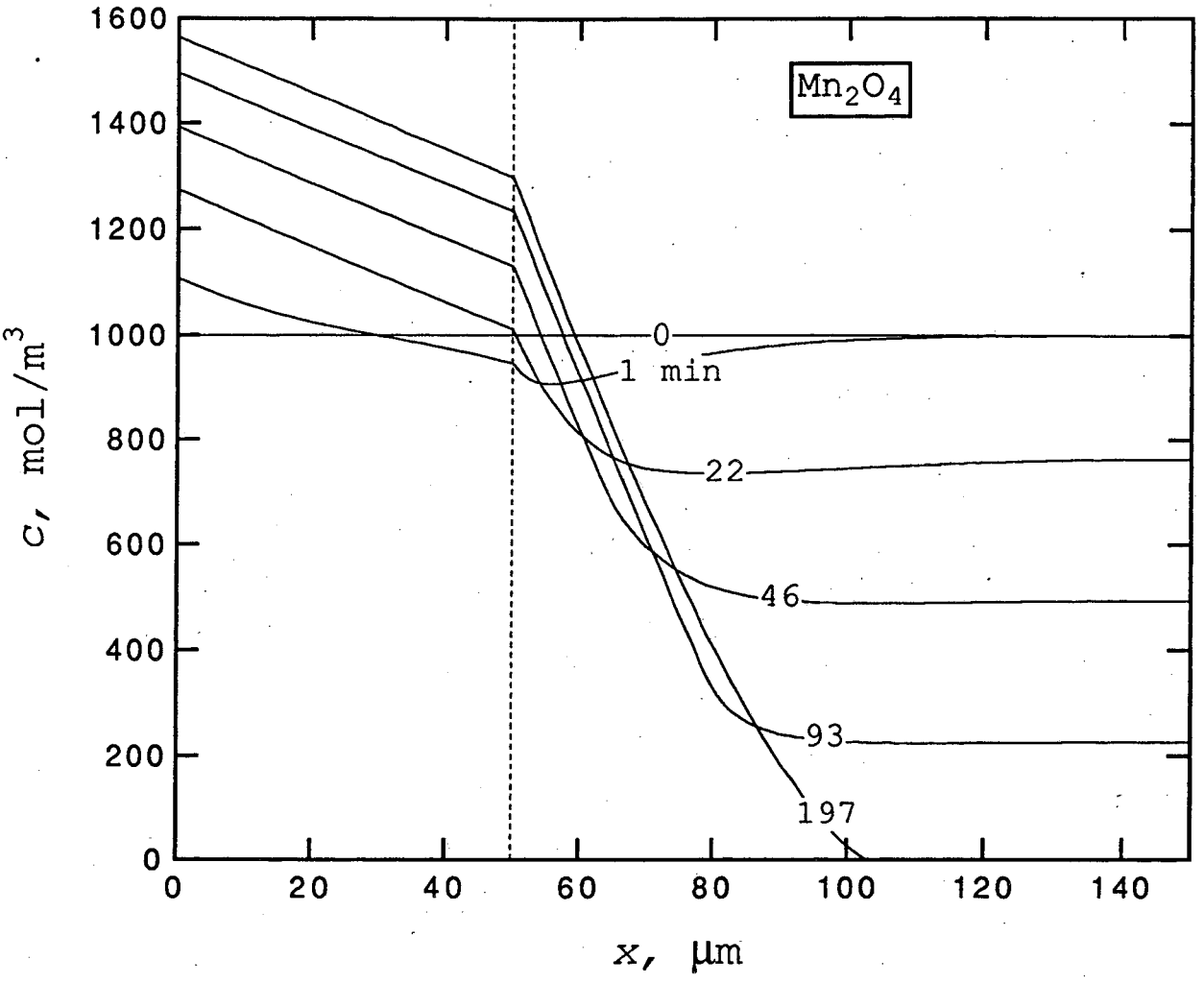

Figure 3. Concentration profiles across the cell during galvanostatic discharge at $I = 5\ A/m^2$. The separator/positive electrode boundary is indicated by a dashed line. Time since the beginning of discharge is given in minutes.

zero. After this time, the remaining active material in the back half of the electrode is no longer accessible. The maximum concentration, which occurs at x=0 for discharge, is less than 1600 mol/m^3 for this system. As this is significantly less than the solubility limit, it does not appear to be a concern in the present system. Concentration profiles can also be developed for lithium inside the manganese dioxide particles at any distance into the positive electrode. However, due to the small size of the particles, the concentration is uniform, and we have not included any of these graphs.

It is also interesting to examine the reaction rate distribution during the course of discharge in this system. In figure 4 we present the divergence of the solution phase current density across the positive electrode at various times during a discharge at I=5 A/m^2. A detailed discussion of current distributions in porous electrodes has been given elsewhere.[11,13] We find a very nonuniform current distribution here, with a spike-like reaction front moving through the electrode. This is expected from consideration of the shape of the open-circuit potential for manganese dioxide coupled with the lack of an appreciable kinetic resistance for the insertion process. A highly sloping open-circuit potential function or an appreciable kinetic resistance will tend to bring about a more uniform current distribution. Examining figure 4, we see that the first reaction front reaches the depleted region of the electrode at about 120 minutes into discharge. At this point, a second, smaller front has already developed and is moving through the electrode behind the first front. This two-front behavior, which has been seen in all of the systems examined here, is a result of the shape of the open-

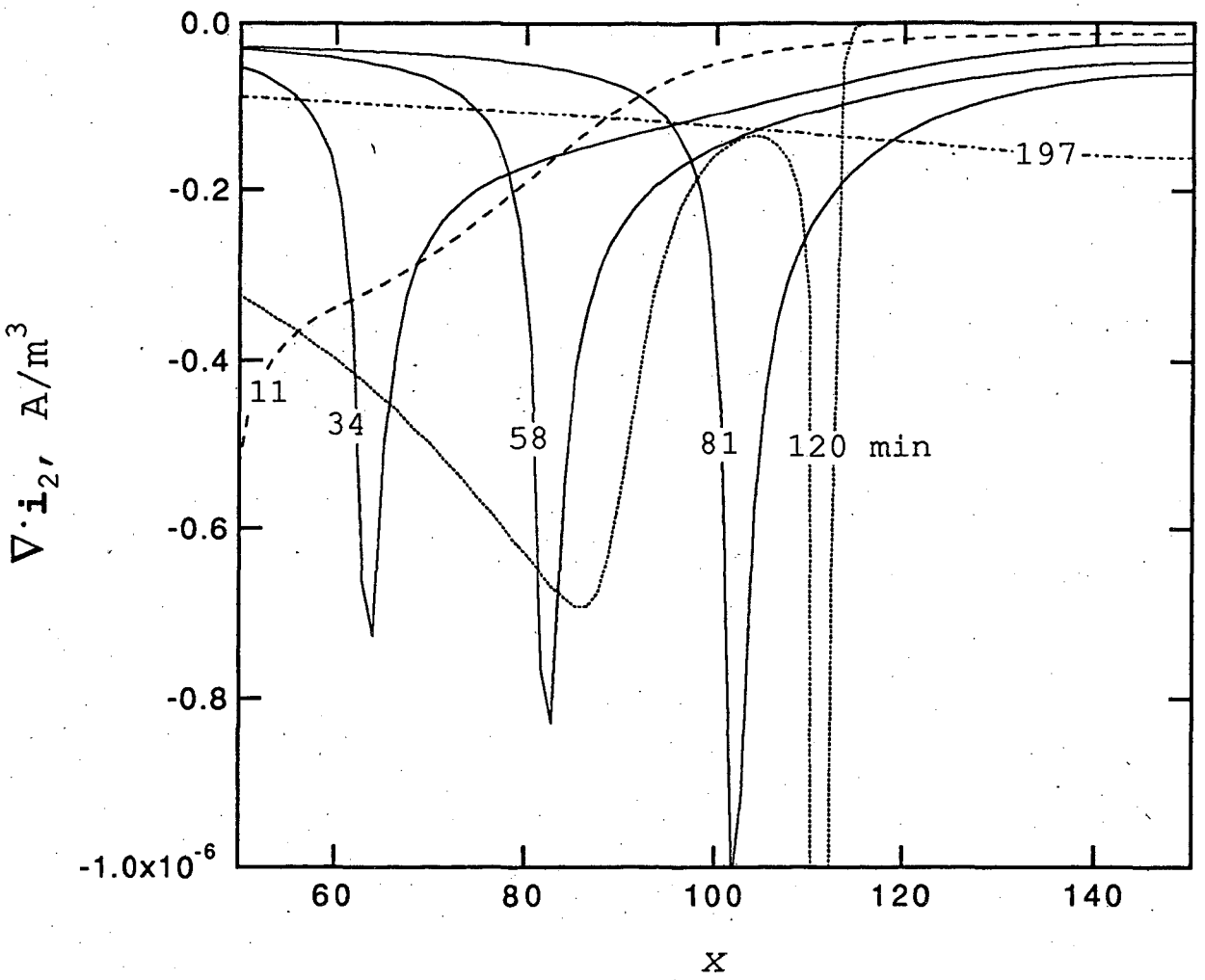

Figure 4. Divergence of solution-phase current density, which is proportional to the pore wall flux of lithium into the positive-electrode active material, during galvanostatic discharge at $I = 5\ A/m^2$. Time since the beginning of discharge is given in minutes. Different line forms are used merely to assist the reader in distinguishing between various curves.

circuit potential *versus* state of charge for manganese dioxide. This curve (see dashed line on figure 2) has two plateaux separated by a small sloped region at approximately y=0.6. The increase in slope at y=0.6 causes the current distribution to become more uniform for a brief period, and after this, the second spike develops.

As we have seen that the primary factor leading to incomplete utilization of active material at higher discharge rates is the concentration gradient that develops, it is interesting to simulate the system in the absence of concentration gradients. We can imagine making t_+^0 approach unity by either allowing D_{0+} to approach infinity or having D_{0-} approach zero (see equation 2). In situations where the anion is fixed to the polymer chain, the latter approach is implied. Notice that setting D_{0-} equal to zero means that the salt diffusion coefficient, given by

$$D = \frac{c_T}{c_0}\left[1 + \frac{\partial \ln f_\pm}{\partial \ln c}\right]\left[\frac{D_{0+}D_{0-}(z_+ - z_-)}{z_+D_{0+} - z_-D_{0-}}\right], \qquad (3)$$

is then also equal to zero. Because of the lack of concentration gradients with t_+^0=1.0, this is not a problem. To demonstrate this, we provide in figure 5 a simulation of the concentration profile at the end of discharge for three systems in which the transference number is approaching unity while simultaneously decreasing the salt diffusion coefficient accordingly. Here we see that, as t_+^0 approaches unity, the concentration profiles disappear, even though D is approaching zero.

In figure 6 we present discharge curves at various current densities for a system identical to the base-case system but with t_+^0=1.0. It

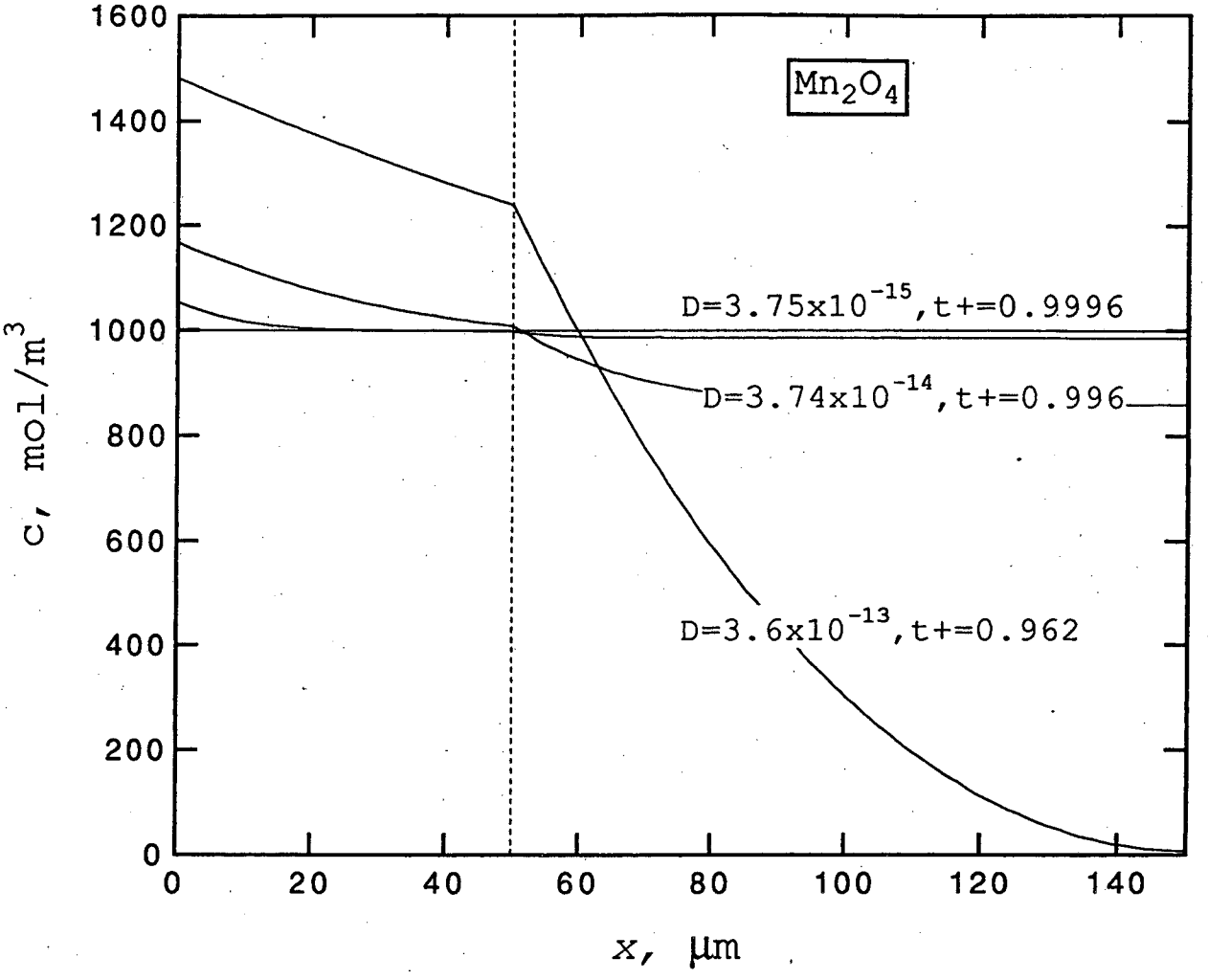

Figure 5. Concentration profiles across the cell at the end of galvanostatic discharges at I = 5 A/m^2 are given. The separator/positive electrode boundary is indicated by a dashed line. System parameters are listed on the figure and given in table 1.

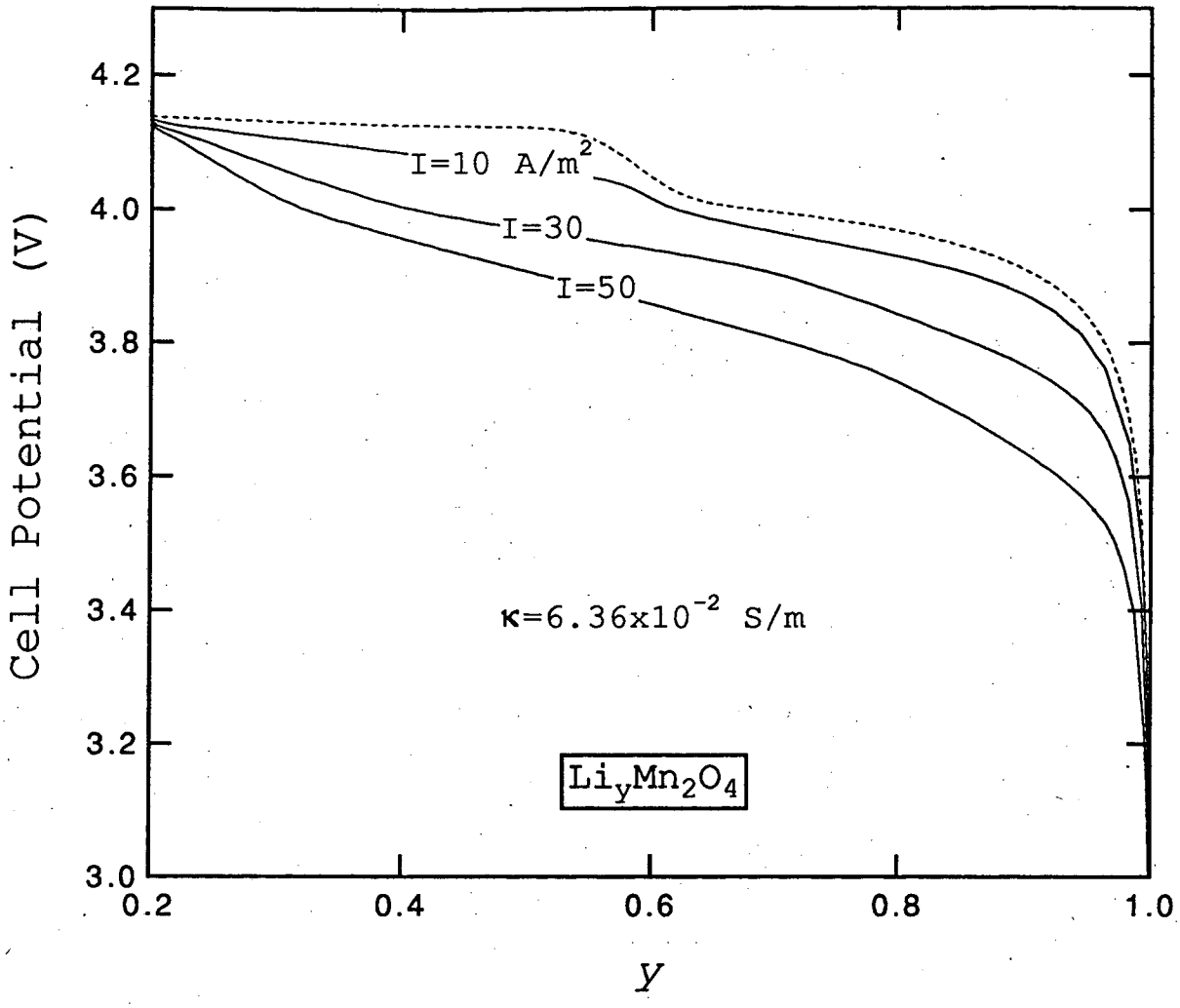

Figure 6. Cell potential *versus* state of charge for a system with unity transference number and no change in conductivity. The dashed line is the open-circuit potential of the cell. Other parameters used in the simulations are given in table 1.

is evident that this system is far superior to the first, with current densities in excess of 50 A/m^2 attainable without any loss of capacity. However, as was discussed previously, it is unlikely that a unity transference number will be obtained in a polymer electrolyte system without an appreciable loss in conductivity. Therefore, the next simulations involve the base-case system, but with the conductivity equal to one-fifth of that above (evaluated at the initial concentration). This loss of conductivity is what would be predicted under dilute solution theory (equation 1).

Figure 7 gives discharge curves for a system with the conductivity reduced to a fifth of its initial value. As before, higher discharge rates are attainable in comparison to the base-case system, but not without increasing ohmic losses in the cell. At I=20 A/m^2, the cell potential drops below the cutoff value (3.0 V) after approximately 93% of the maximum capacity has been utilized. The major source of overpotential in this system is the ohmic drop, which increases over the course of discharge as the reaction front propagates into the back of the cathode; lithium ions must travel farther in the solution phase to reach the reaction front.[16] This also causes the discharge curves to be increasingly sloped at higher discharge rates, which is considered to be a disadvantage for many applications. Since we assumed facile kinetics and a small particle size in the positive electrode (see table 1), surface overpotential and concentration polarization in the interior of the positive electrode particles make very small contributions to the overpotential, even at large discharge rates.

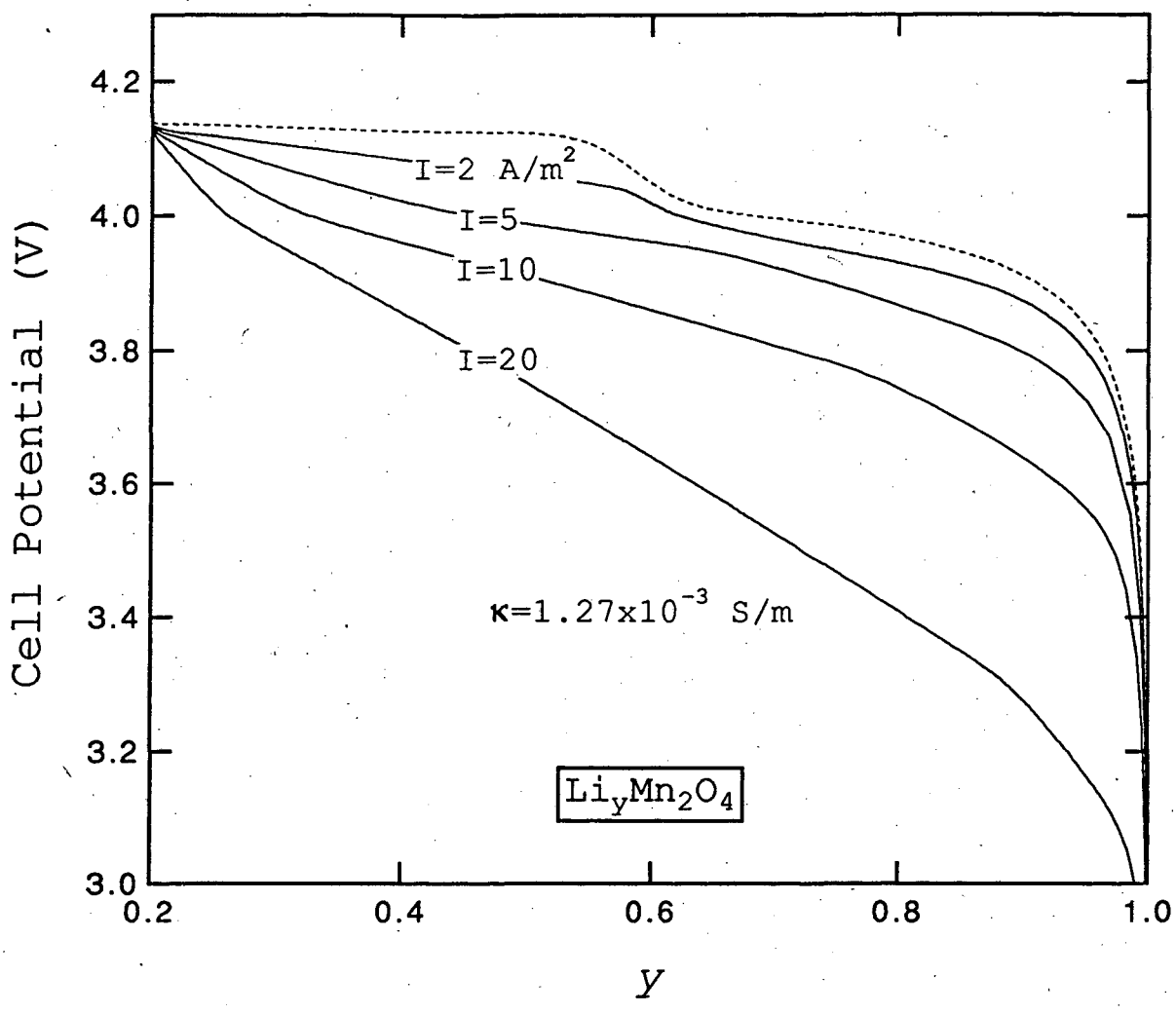

Figure 7. Cell potential *versus* state of charge for a system with unity transference number and one-fifth the conductivity. The dashed line is the open-circuit potential of the cell. Other parameters used in the simulations are given in table 1.

At this point it seems that immobilizing the anion and attaining a unity transference number greatly enhances the performance of these systems. However, a decrease in the conductivity of only 80%, the dilute solution result, has proved very difficult to obtain. Generally, decreases have been between one and two orders of magnitude for systems with a unity transference number.[5,7] This is just another confirmation of the concentrated nature of lithium salt/polymer solutions, which has been demonstrated from the concentration dependence of transport properties,[17] activity-coefficient corrections,[3] and theoretical and experimental studies of ion pairing in these systems.[18,19] Under concentrated solution theory, we find a different expression for the conductivity, which includes a term accounting for ion-ion interactions ignored in the dilute solution treatment.

$$\frac{1}{\kappa} = \frac{-RT}{c_T z_+ z_- F^2}\left(\frac{1}{D_\pm} - \frac{c_0 z_-}{c_+(z_+ D_{0+} - z_- D_{0-})}\right) . \qquad (4)$$

Ion-ion interactions are treated with the pairwise interaction parameter, $D_\pm$, whose concentration dependence has been discussed by several authors.[11,20,21]

As stated before, in concentrated solutions we have $n(n-1)/2$ transport properties, where n is the number of independent species. For systems such as a lithium salt/polymer solvent, *e.g.* $LiCF_3SO_3$ in polyethylene oxide, the exact species that exist under given conditions may be complicated by the existence of ion-pairs and other aggregate species. However, as long as these exchange processes are fast enough to be in equilibrium on time scales of interest, only three independent

species exist, and the rest of the species concentrations are related through equilibrium expressions. Although several choices exist, it is easiest to take the three species in the above solution to be Li^+, $CF_3SO_3^-$, and the polymer. Then the conductivity, lithium ion transference number, and salt diffusion coefficient describe the transport processes exactly, with the concentration dependence of these properties accounting for the various species that may actually exist.

Along the above lines, we have carried out simulations with the conductivity reduced to a tenth of the initial value. In figure 8 we present the discharge curves for this system. The trend seen in going from figure 6 to figure 7 continues here, with even larger ohmic drops caused by the smaller conductivity and nonuniform current distribution. In this case, at I=20 A/m^2, the cell potential drops below the cutoff value at y=0.69. This system is able to attain 100% utilization at current densities up to 10 A/m^2, still significantly better than the base case, for which $t_+^0 \neq 1.0$.

Decreases in conductivity of greater than an order of magnitude have also been explored here. We have simulated the discharge behavior of systems with continuously decreasing values of the conductivity for a single value of the current, I=5 A/m^2. Several of these discharge curves are presented in figure 9, where it is evident that there exists a value of the conductivity below which the system performs more poorly, on the basis of material utilization, than the initial system with nonunity transference number (compare with figure 2). In order to quantify the comparison, we can calculate the energy densities and, after this, the peak power densities that are attainable with each system.

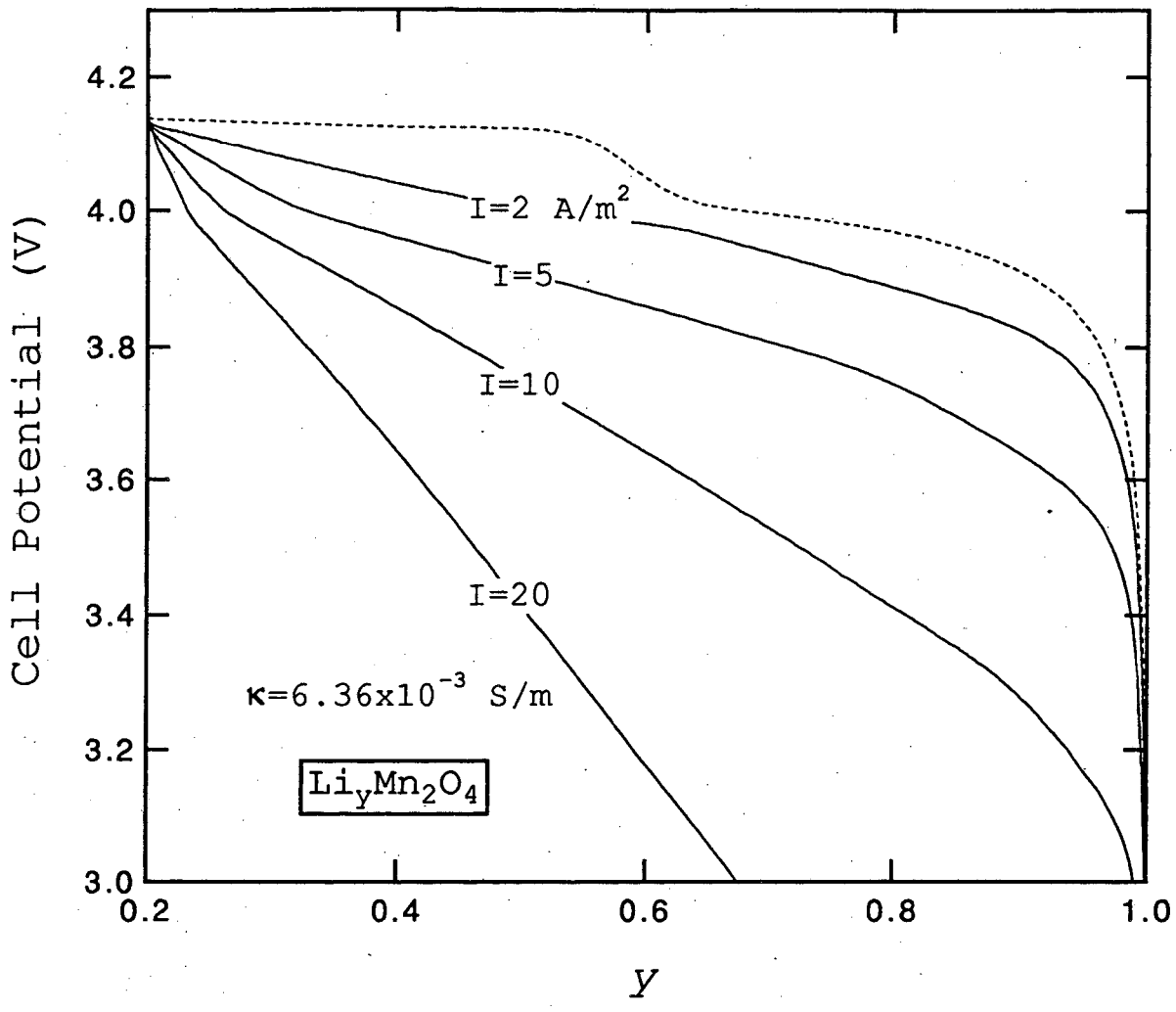

Figure 8. Cell potential *versus* state of charge for a system with unity transference number and one-tenth the conductivity. The dashed line is the open-circuit potential of the cell. Other parameters used in the simulations are given in table 1.

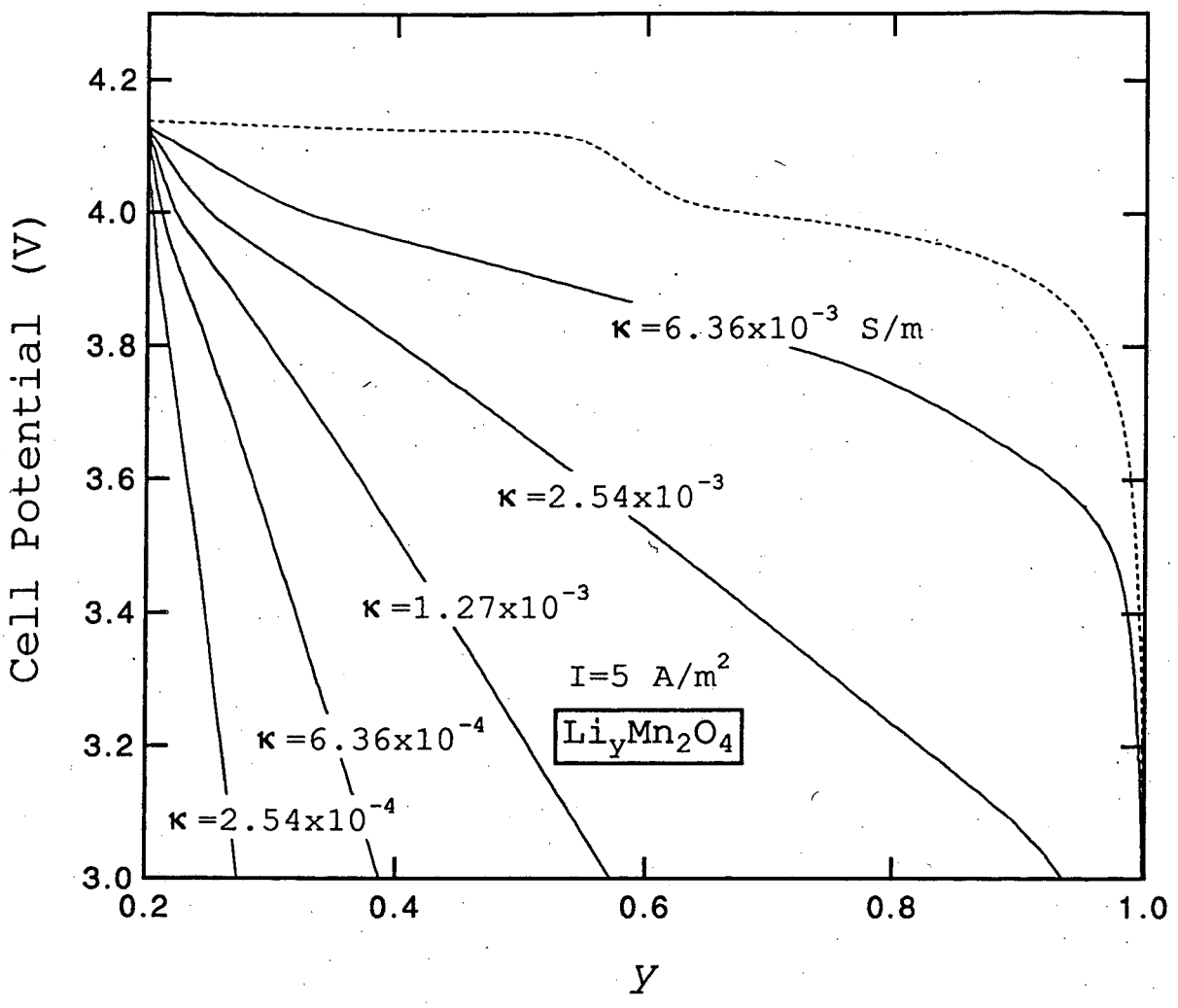

Figure 9. Cell potential *versus* state of charge for a system with unity transference number and various values of the conductivity. The cell is discharged at I = 5 A/m^2. The dashed line is the open-circuit potential of the cell. Other parameters used in the simulations are given in table 1.

In figure 10 we have prepared a Ragone-type plot, which gives the average specific power *versus* the specific energy for each of the above systems. The mass of the system includes the separator and both electrodes, but not additional battery masses such as current collectors and casing. The density of $PEO_nLiCF_3SO_3$ is taken to be 1.2 g/cm^3, independent of the concentration, and the density of inert filler material is taken to be 2.0 g/cm^3. Note that the maximum specific energy is not affected by varying the transport parameters, which is the expected result, and approaches the theoretical value based on the maximum capacity of $LiMn_2O_4$ and the system parameters. The solid lines represent systems with a unity transference number, while the dashed line is the base-case system with a nonunity transference number. This figure serves to quantify the effect seen earlier, which is that as the discharge rate increases, the material utilization is improved for systems with t_+^0=1.0 and similar conductivity. However, we can see from figure 10 that when $\kappa<2.54\times10^{-3}$ S/m, the systems with unity transference number are no longer obtaining higher utilizations than the base case. This transition occurs when the conductivity has been reduced to approximately 2.7% of its initial value. For applications with lower discharge rates, where concentration gradients are not severe, decreases in the conductivity can be the major source of overpotential. This is apparent at very low values of the power (below approximately 25 W/kg), where the energy is higher for the base-case system with nonunity transference number.

In addition to the average specific power, it is interesting to examine the peak specific power that the system can provide. We calcu-

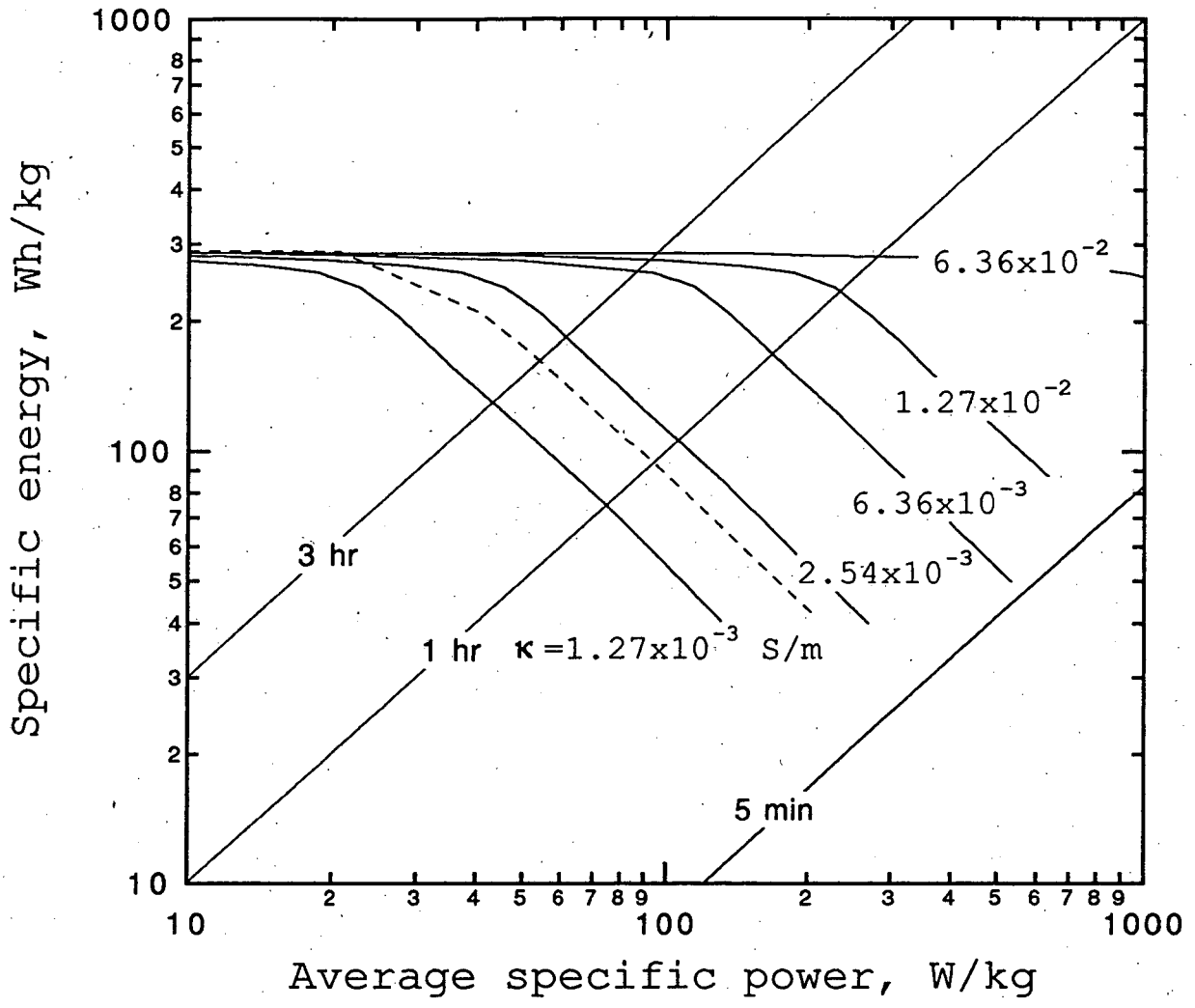

Figure 10. Ragone plot for the lithium/manganese dioxide system. The conductivity of the electrolyte is a parameter. Other parameters used in the simulations are given in table 1. The dashed line is a system with nonunity transference number.

late the power available for a thirty-second pulse of current at various depths of discharge. The percent depth of discharge (%DOD) is based on the maximum capacity that the system can attain before the potential drops below the cutoff value. The initial discharge is carried out at I=5 A/m^2, giving a 5.6-hour discharge time. The specific power for the base case is given in figure 11 at 20, 40, 60, and 80% DOD. From this we calculate the peak power to be, for example, 269.7 W/kg at 40% DOD. The peak power is, in general, strongly dependent on the depth of discharge.

To compare with systems having a unity transference number, in figure 12 we present the power available at 40% DOD for several different values of the conductivity. As with the specific energy, the conductivity can be decreased substantially before the peak power drops below that of the base-case system. However, when the conductivity decreases below approximately 6.1×10^{-3} S/m, the system with nonunity transference number becomes superior. This transition occurs earlier from considerations of the peak power than it did from the analysis of the specific energy. At first this may seem to contradict the conclusion drawn from the specific energy comparison, that at higher discharge rates a unity transference number makes a substantial improvement in the system. However, in the present case the discharge time is so short (30 seconds), that concentration gradients are barely given time to establish. This is in contrast to the ohmic drop, which is established immediately and thus has a large impact on the peak power. As is apparent from figure 12, small decreases in the conductivity bring about very large decreases in the peak power.

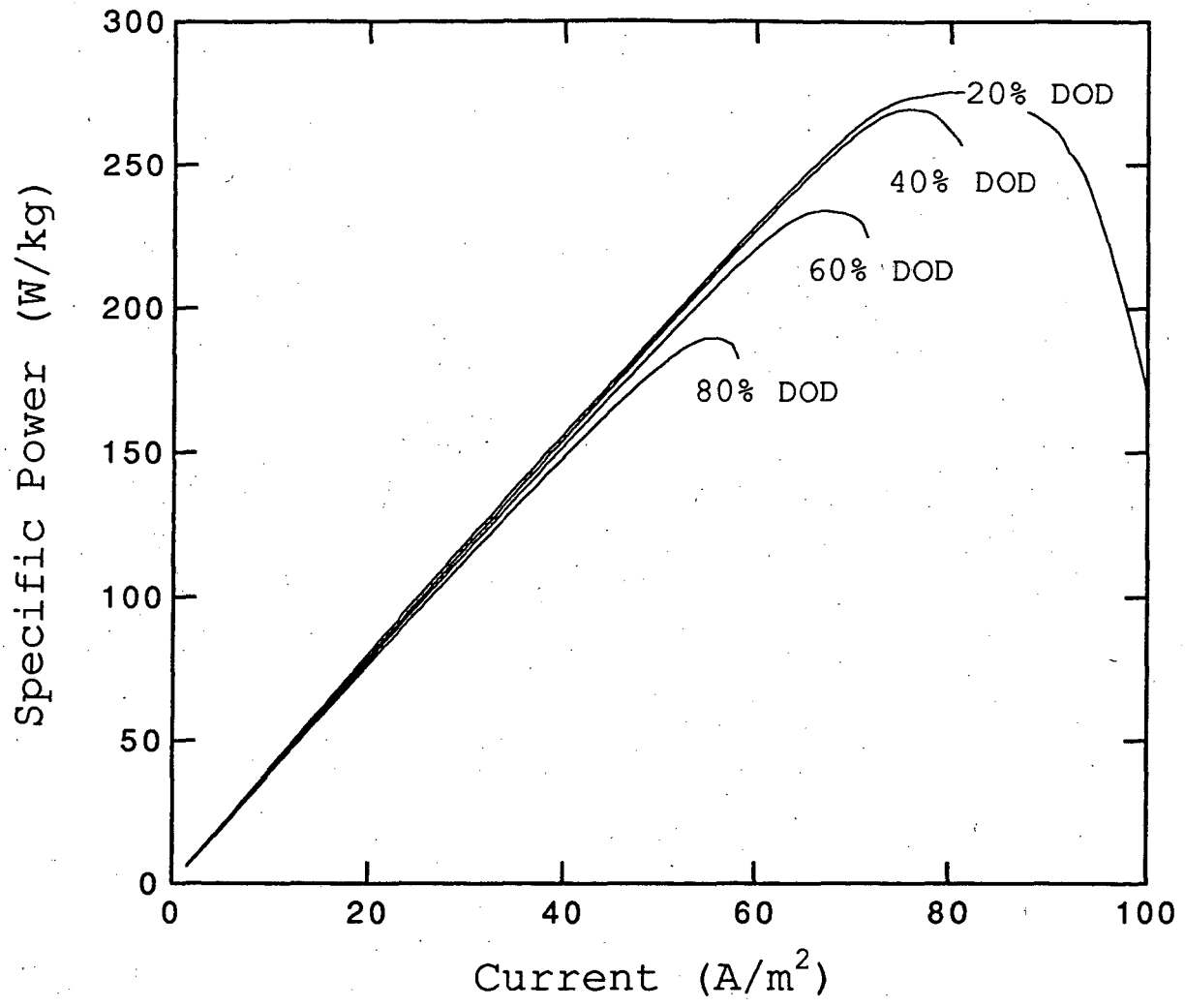

Figure 11. The power available at various depths of discharge is given *versus* discharge rate for the lithium /manganese dioxide system. This system has a nonunity transference number. Other parameters used in the simulations are given in table 1.

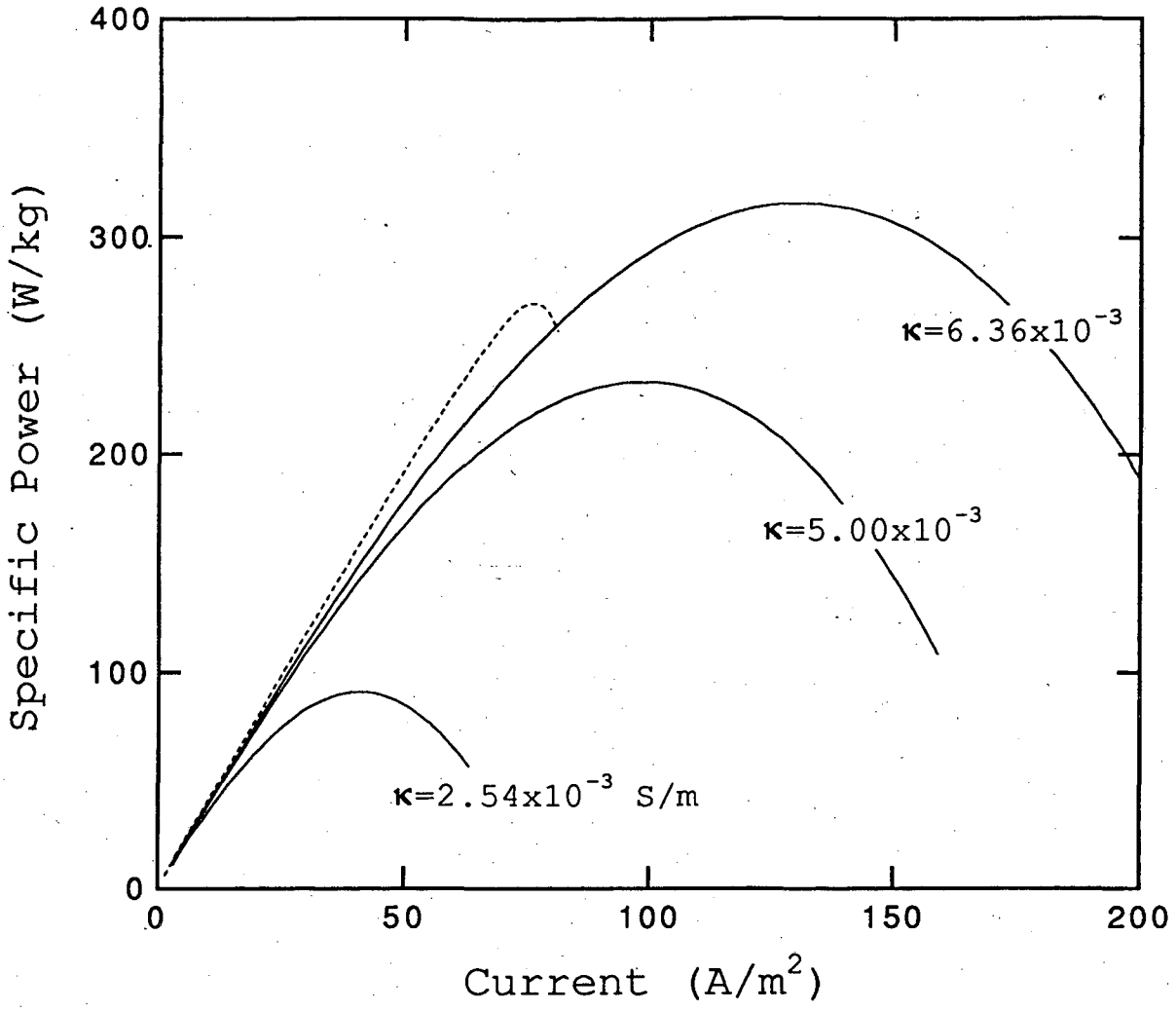

Figure 12. The power at 40% depth of discharge is given *versus* discharge rate for the lithium/manganese dioxide system. The conductivity of the separator is a parameter. The dashed line is the system with nonunity transference number. Other parameters used in the simulations are given in table 1.

One last difference between these systems is seen when examining the peak power as a function of the percent depth of discharge. In all cases the peak power available decreases as discharge proceeds, indicating the increased difficulty in accessing active material. In figure 13 we show the peak power *versus* %DOD for several systems with unity transference number and various conductivities, compared with the base-case system. Again, the 30-s power peaks are performed at various points in a constant-current discharge at 5 A/m^2. The peak power available for the base case is substantially reduced due to the nonunity transference number; notice that the curves with unity transference number given in figure 13 all have lower values of the conductivity than the base case. However, the base-case peak power is almost constant *versus* depth of discharge, indicating that the impact of a nonunity transference number on the peak power is similar at all points during the discharge. This is in contrast to the unity transference number systems, whose peak power is substantially reduced as the depth of discharge increases. In these systems the peak power steadily decreases because the ohmic drop steadily increases as discharge proceeds, caused by the larger distance that ions must travel to reach the reaction front (see discussion of figure 7). The comparison of peak power values made in figure 12 thus depends on the depth of discharge, and farther into discharge the base-case system's peak power performance improves compared to the other systems.

A final issue related to the transference number that can be clarified involves values of t_+^0 less than or equal to zero. This has been discussed previously in the literature, and it has been stated that a

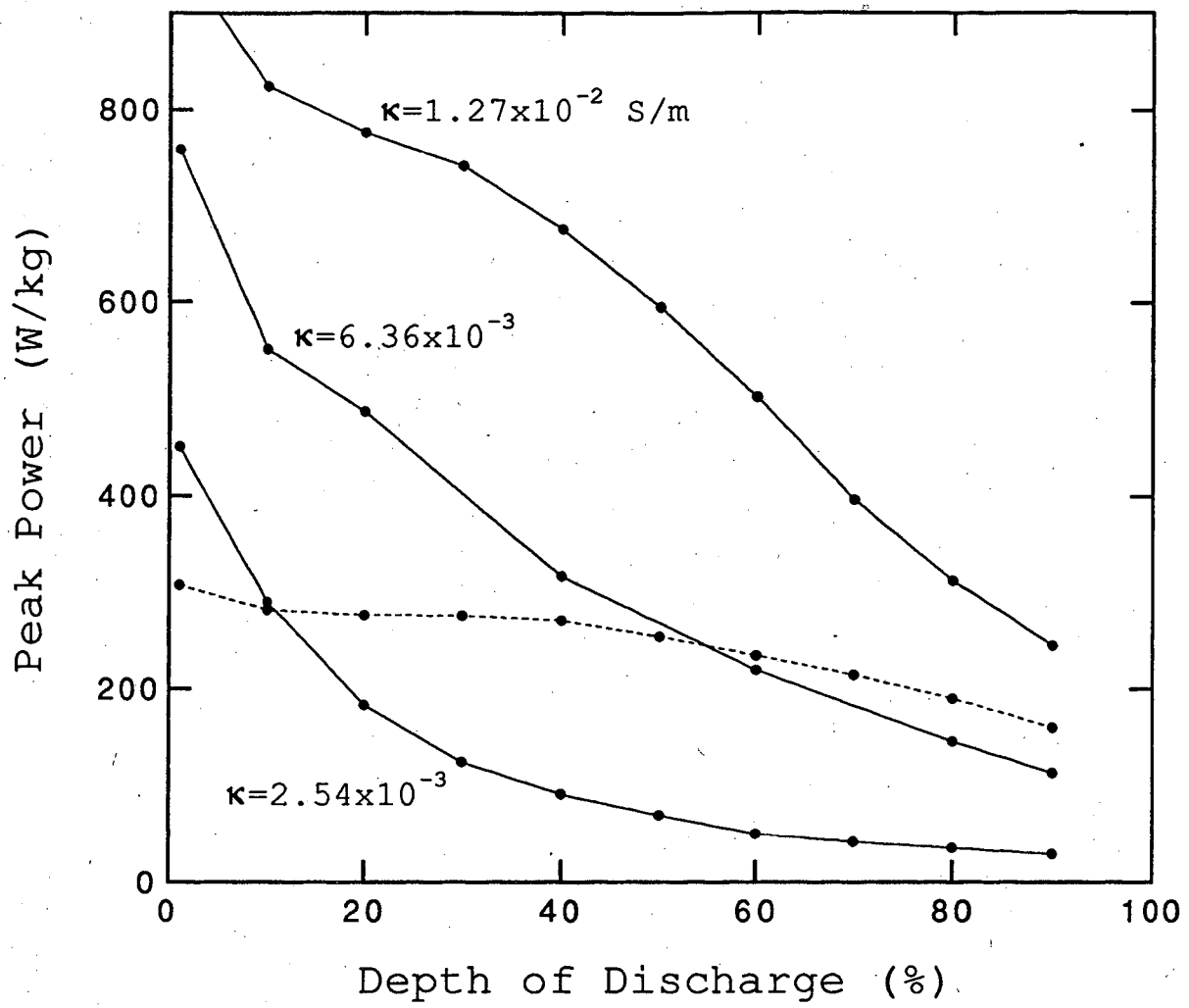

Figure 13. The peak power is given *versus* depth of discharge for the lithium/manganese dioxide system. The dashed line is the system with nonunity transference number (having initially the conductivity of 6.36×10^{-2} S/m). The other lines are for systems with unity transference number and various conductivities. Other parameters used in the simulations are given in table 1.

zero transference number for the lithium ion does not mean that a system is inoperable.[22] Under the framework presented above, we can see that the transference number can become zero if either D_{0+} is equal to zero or if D_{0-} approaches infinity (see equation 2). In the former case, the salt diffusion coefficient is also equal to zero (equation 3), and the concentration profile that develops has an infinite gradient, leading to immediate failure of the cell. In the latter case, the salt diffusion coefficient will equal twice the cation diffusion coefficient $2D_{0+}$, and the system can operate sucessfully, albeit with a large concentration gradient. The steady-state concentration gradient in the separator during discharge is given by

$$\Delta c \approx \frac{I(1-t_+^0)L}{FD} \quad . \tag{5}$$

Hence for t_+^0 equal to zero a large gradient is expected. We can also see that values of t_+^0 less than zero will lead to increasingly larger concentration gradients in the cell. This will, of course, negatively impact the performance of the system, but it will not necessarily cause the cell to fail. At low discharge rates, a system with a negative transference number for the lithium ion could still operate sucessfully.

It is tempting to ascribe a negative transference number to the existence of mobile complex species, such as negatively charged triplet ions.[19] However, given only data on the transport properties, it is impossible to surmise which species actually exist in solution at a given concentration. To do this would require equilibrium data obtained, for example, by spectroscopic methods.[23] Yet, as previously

discussed, for the present purpose of modeling the behavior of these cells, only the three concentration dependent transport properties are necessary to describe completely the solution phase.

Conclusions

The discharge rates of cells using lithium salts solvated with polymer electrolytes are limited by depletion of the electrolyte in the porous electrode. This problem does not exist in polymers with a unity transference number for the lithium ion, attained for example by attaching the anion to the polymer chain. However, decreases in the conductivity that result from this situation can cancel the improvements derived from the unity transference number. We have used one particular system, that of lithium/$PEO_nLiCF_3SO_3$/manganese dioxide, to demonstrate the tradeoff that exists between these parameters.

At very low discharge rates, when the steady-state concentration gradient is not large enough to deplete the solution of electrolyte, no improvement is gained from a unity transference number. But in applications where a high discharge rate is desired, such as electric vehicles, a unity transference number leads to substantial improvements in material utilization. This is true even when the conductivity is reduced by over an order of magnitude, down as far as to 2.7% of its initial value. The peak power available for a thirty-second pulse of current is also improved for systems with unity transference number, although this is strongly dependent on the depth of discharge, and the improvements are not as significant as with the specific energy. The peak power for systems with unity transference number steadily decreases as the discharge proceeds due to an increasing ohmic drop as the

reaction front penetrates into the depths of the porous electrode. This is in constrast to the base-case system, indicating that the effect of a nonunity transference number on the peak power, although drastic, is roughly constant as discharge proceeds. At 40% depth of discharge, improvements in the peak power occur until the conductivity is reduced to 9.6% of its initial value.

It must be realized that specific numerical results presented here are a strong function of the particular system chosen for study. For this reason the discussion of results, when possible, has been generalized to apply to any of the lithium salt/polymer electrolyte combinations that exist. In general, we find that improvements made by having a unity transference number will depend on the intended application for the system. For applications with moderately high discharge rates, such as electric vehicles, the advantage of a unity transference number is greatest. This advantage may still exist when the conductivity is decreased by up to an order of magnitude.

Acknowledgements

This work was supported by the Assistant Secretary for Conservation and Renewable Energy, Office of Transportation Technologies, Electric and Hybrid Propulsion Division of the U. S. Department of Energy under Contract No. DE-AC03-76SF00098.

Appendix A Summary of model equations

The model can be divided into the separator and composite cathode regions. In the solution phase of the composite cathode the equations are

$$\epsilon\frac{\partial c}{\partial t} = \nabla\cdot\left(\epsilon D\nabla c\right) - \frac{\mathbf{i}_2\cdot\nabla t_+^0}{z_+\nu_+F} + \frac{aj_n\left(1-t_+^0\right)}{\nu_+}, \tag{A-1}$$

$$\mathbf{i}_2 = -\kappa\nabla\Phi_2 + \frac{\kappa RT}{F}\left(1+\frac{\partial \ln f_{\pm}}{\partial \ln c}\right)\left(1-t_+^0\right)\nabla\ln c, \tag{A-2}$$

$$aj_n = \frac{-s_i}{nF}\nabla\cdot\mathbf{i}_2. \tag{A-3}$$

In the solid phase of the composite cathode

$$\mathbf{i}_1 = -\sigma\nabla\Phi_1, \tag{A-4}$$

$$\frac{\partial c_s}{\partial t} = D_s\left[\frac{\partial^2 c_s}{\partial r^2} + \frac{2}{r}\frac{\partial c_s}{\partial r}\right]. \tag{A-5}$$

These two phases are related through the boundary condition

$$j_n = -D_s\frac{\partial c_s}{\partial r} \text{ at } r=R_s, \tag{A-6}$$

as well as a Butler-Volmer kinetics expression. In the separator region the first two equations apply with j_n=0.0 and ϵ=1.0.

These equations are linearized and solved simultaneously using the subroutine BAND.[11] We have two independent variables (x and t) and six dependent variables (c, Φ_2, c_s, i_2, j_n, and Φ_1). The Crank-Nicolson implicit method was used to evaluate the time derivatives.

Appendix B Transport properties of the electrolyte and thermodynamic data

Polyethylene oxide, 1 M $LiCF_3SO_3$. — The concentration dependence of the conductivity was taken from available data in the literature and was fit to a polynomial.[24] The concentration dependence of the transference number was fit to the equation:[3]

$$t_+^0 = 0.0107907 + 1.48837\text{x}10^{-4}c \ .$$

The concentration dependence of the diffusion coefficient was not available, so it was taken to have the constant value $7.5\text{x}10^{-12}$ m^2/sec.[3] Activity coefficient data have not been reported.

The exchange current density for the lithium/PEO interface, including the concentration dependence, is taken from the literature.[15] This value, based on initial conditions, is $i_{o,1}$=12.6 A/m^2. The transfer coefficients are each taken to be 0.5.

Electrode thermodynamic data. — The open-circuit potential versus state of charge for manganese dioxide was fit from data in the literature.[25] This fit[26] is used to generate the dashed curve on the simulated discharge curves presented here.

List of Symbols

a	specific interfacial area, m^2/m^3
c	concentration of electrolyte, mol/m^3
c_0	concentration of solvent, mol/m^3
c_T	total concentration of solution, mol/m^3
D, D_s	diffusion coefficient of electrolyte and of lithium in the solid matrix, m^2/s
D_i	dilute solution diffusion coefficient of species i through solvent, m^2/s
D_{ij}	pairwise interaction parameter between species i and j, m^2/s
$f_{\pm}$	mean molar activity coefficient
F	Faraday's constant, 96,487 C/eq
i	current density, A/m^2
i_o	exchange current density, A/m^2
I	superficial current density, A/m^2
j_n	pore wall flux across interface, $mol/m^2 \cdot s$
L	total cell thickness, m
r	radial distance in a particle of active material, m
R	universal gas constant, 8.3143 J/mol·K
R_s	radius of positive electrode particles, m
s_i	stoichiometric coefficient of species i
t	time, s
t_i^0	transference number of species i
T	temperature, K
x	distance from the negative electrode, m

z_i	charge number of species i
α_a, α_c	transfer coefficients
δ_s	thickness of separator, m
δ_+	thickness of composite positive electrode, m
ϵ	porosity
κ	conductivity of the electrolyte, S/m
ν_+, ν_-	number of cations and anions into which a mole of electrolyte dissociates
ρ_s	density of solid material, kg/m^3
σ	conductivity of the solid composite electrode, S/m
Φ	electrical potential, V

Subscripts

f	filler
s	solid phase or separator
0	solvent
1	solid matrix
2	solution phase
t	concentration in intercalation material for y=1
+	positive electrode or cation
-	negative electrode or anion

Superscripts

0	initial condition

References

[1] F. M. Gray, *Solid Polymer Electrolytes*, VCH, New York, NY (1991).

[2] P. R. Sorensen and T. Jacobsen, "Limiting Currents In The Polymer Electrolyte: $PEO_xLiCF_3SO_3$," *S. S. Ionics*, 9&10, 1147 (1983).

[3] A. Bouridah, F. Dalard, D. Deroo, and M. Armand, "Potentiometric Measurements of Ionic Transport Parameters in Poly(Ethylene Oxide)-LiX Electrolytes," *J. Appl. Electrochem.*, 17, 625 (1987).

[4] M. Leveque, J. F. LeNest, A. Gandini, and H. Cheradame, "Ionic Transport Numbers in Polyether Networks Containing Different Metal Salts," *Makromol. Chem., Rapid Commun.*, 4, 497 (1983).

[5] N. Kobayashi, M. Uchiyama, and E. Tsuchida, "Poly(Lithium Methacrylate-Co-Oligo(Oxyethylene)Methacrylate) as a Solid Electrolyte with High Ionic Conductivity," *S. S. Ionics*, 17, 307 (1985).

[6] L. C. Hardy and D. F. Shriver, "Preparation and Electrical Response of Solid Polymer Electrolytes with Only One Mobile Species," *J. Am. Chem. Soc.*, 107, 3823 (1985).

[7] M. Watanabe, S. Nagano, K. Sanui and N. Ogata, "Estimation of the Lithium Ion Transport Number in Polymer Electrolytes by the Combination of Complex Impedance and Potentiostatic Polarization Measurements," *S. S. Ionics*, 28-30, 911 (1988).

[8] Z. Ogumi, Y. Uchimoto, Z. Takehara, and F. R. Foulkes, "Ionically Conductive Thin Polymer Films Prepared by Plasma Polymerization,"

J. Electrochem. Soc., 137, 29 (1990).

[9] D. J. Bannister, G. R. Davies, I. M. Ward, and J. E. McIntyre, "Ionic Conductivities for Poly(ethylene Oxide) Complexes with Lithium Salts of Monobasic and Dibasic Acids and Blends of Poly(ethylene Oxide) with Lithium Salts of Anionic Polymers," *Polymer*, 25, 1291 (1984).

[10] M. Armand, "Polymer Solid Electrolytes: An Overview," *S. S. Ionics*, 9&10, 745 (1983).

[11] J. Newman, *Electrochemical Systems*, Prentice Hall, Englewood Cliffs, New Jersey (1991).

[12] R. A. Robinson and R. H. Stokes, *Electrolyte Solutions*, p. 161, Butterworths, London, 2nd. Ed. (1959).

[13] M. Doyle, T. F. Fuller, and J. Newman, "Modeling of the Galvanostatic Charge and Discharge of the Lithium/polymer/insertion Cell," *J. Electrochem. Soc.*, 140, 1526 (1993).

[14] D. Guyomard and J. M. Tarascon, "Li Metal-Free Rechargeable $LiMn_2O_4$/Carbon Cells: Their Understanding and Optimization," *J. Electrochem. Soc.*, 139, 937 (1992).

[15] C. A. C. Sequeira and A. Hooper, "The Study of Lithium Electrode Reversibility Against PEO-$LiCF_3SO_3$ Polymeric Electrolytes," *Solid State Ionics*, 9&10, 1131 (1983).

[16] W. Tiedemann and J. Newman, "Maximum Effective Capacity in an Ohmically Limited Porous Electrode," *J. Electrochem. Soc.*, 122, 1482 (1975).

[17] C. D. Robitaille and D. Fauteux, "Phase Diagrams and Conductivity Characterization of Some PEO-LiX Electrolytes," *J. Electrochem. Soc.*, 133, 315 (1986).

[18] M. A. Ratner, "Aspects of the Theoretical Treatment of Polymer Solid Electrolytes: Transport Theory and Models," in *Polymer Electrolyte Reviews-1*, ed. J. R. MacCallum and C. A. Vincent, Elsevier Applied Science, London (1987).

[19] P. G. Bruce and C. A. Vincent, "Effect of Ion Association on Transport in Polymer Electrolytes," *Far. Disc. Chem. Soc.*, 88, 43 (1988).

[20] T. W. Chapman, "The Transport Properties of Concentrated Electrolyte Solutions," Ph.D. thesis, Univ. of California, Berkeley (1967).

[21] S. Umino and J. Newman, "Diffusion of Sulfuric Acid in Concentrated Solutions," *J. Electrochem. Soc.*, 140, 2217 (1993).

[22] G. G. Cameron, J. L. Harvie, and M. D. Ingram, "The Steady State Current and Transference Number Measurements in Polymer Electrolytes," *S. S. Ionics*, 34, 65 (1989).

[23] M. Dakihana, S. Schantz, and L. M. Torell, "Raman Spectroscopic Study of Ion-Ion Interaction and its Temperature Dependence in a Poly(propylene-oxide)-based $NaCF_3SO_3$-Polymer Electrolyte," *J. Chem. Phys.*, 92, 6271 (1990).

[24] D. Fauteux, "Lithium Electrode/PEO-Based Polymer Electrolyte Interface Behavior Between 60° and 120°C," *J. Electrochem. Soc.*, 135,

2231 (1988).

[25] T. Ohzuku, M. Kitagawa, and T. Hirai, "Electrochemistry of Manganese Dioxide in Lithium Nonaqueous Cell," *J. Electrochem. Soc.*, 137, 769 (1990).

[26] T. F. Fuller, M. Doyle, and J. Newman, "Simulation and Optimization of the Dual Lithium Ion Insertion Cell," submitted to *J. Electrochem. Soc.*, May 1993.

LAWRENCE BERKELEY LABORATORY
UNIVERSITY OF CALIFORNIA
TECHNICAL INFORMATION DEPARTMENT
BERKELEY, CALIFORNIA 94720